PURE-MRI: An International Study Assessing Physician Accuracy in Delineating the Prostate and Urethra on Prostate MRI

Lily Nguyen[1,2], Yuze Song[1,3], Anna Dornisch[1], Madison Baxter[1], Tristan Barrett[4], Anders M Dale[5], Mukesh Harisinghani[6], Sophia C Kamran[7], Michael A Liss[8], Robert T Dess[9], Daniel JA Margolis[10], Eric P Weinberg[11], and Tyler M Seibert[1,5,8,12]

[1]*Department of Radiation Medicine and Applied Sciences, University of California San Diego, La Jolla, CA*
[2]*University of California San Diego School of Medicine, La Jolla, CA*
[3]*Department of Electrical and Computer Engineering, University of California San Diego, La Jolla, CA*
[4]*Department of Radiology, University of Cambridge, Cambridge, United Kingdom*
[5]*Department of Radiology, University of California San Diego, La Jolla, CA*
[6]*Department of Radiology, Massachusetts General Hospital, Boston, MA*
[7]*Department of Radiation Oncology, Massachusetts General Hospital, Harvard Medical School, Boston, MA*
[8]*Department of Urology, University of California San Diego, La Jolla, CA*
[9]*Department of Radiation Oncology, University of Michigan, Ann Arbor, MI*
[10]*Department of Radiology, Cornell University, Ithaca, NY*
[11]*Department of Clinical Imaging Sciences, University of Rochester Medical Center, Rochester, NY*
[12]*Department of Bioengineering, University of California San Diego, La Jolla, CA*

Abstract:

Purpose/Objective(s): Precise delineation of genitourinary (GU) structures during prostate cancer (PCa) care is critical to optimize treatment delivery while minimizing toxicity and injury. The Prostate and UREthra on MRI (PURE-MRI) study was an international, prospective study to assess physicians' accuracy segmenting the prostate and urethra on MRI.

Materials/Methods: Physicians who diagnose or treat PCa were invited to contour the prostate and urethra on up to 4 patient cases using standard T_2-weighted MRI (all planes). We compared these contours to reference consensus segmentations produced by a multidisciplinary panel of experts. We also evaluated the performance of a validated prostate auto-segmentation AI tool. Contour accuracy was assessed with Dice score, deviation from boundary (mm), absolute volume difference (%), and overlap (%). A mixed effects model was used to evaluate potential associations between contour performance and physician specialty, GU focus, or clinical experience.

Results: 62 radiation oncologists, radiologists, and urologists from 11 countries created a total of 224 structure segmentations (114 prostate and 110 urethra contours). Median (min, max) Dice score for the prostate was 0.92 (0.62, 0.95) for physicians. There was no clear effect of clinical experience or focus. Maximum deviation inside (cutting into expert contour), maximum deviation outside (extending beyond expert contour), and mean deviation (per case) from the reference prostate were 3.4 mm (1.0, 12.4), 5.3 mm (2.4, 17.3), and 1.6 mm (0.9, 3.9), respectively. By comparison, the prostate auto-segmentation tool had Dice score, max deviation inside, max distance outside, and mean deviation per case of 0.95 (0.94, 0.96), 3.0 mm, 3.9 mm (3.1, 4.9), and 1.2 mm (1.1, 1.6), respectively. Physician performance was considerably worse for the urethra, with Dice score of 0.33 (0.03, 0.69). No AI tool was tested for the urethra.

Conclusion: Physicians contour the prostate on MRI with overall Dice score >0.9, though contours typically had at least one error >5 mm and sometimes >10 mm. These patterns were observed regardless of clinical experience, specialty, or clinical focus. The AI tool performs well enough for clinical use, given comparable accuracy to practicing physicians. In contrast, urethra segmentation on MRI is challenging. More training, better imaging, and/or AI tools may be necessary to achieve accurate and consistent results for the urethra.

Introduction:

Magnetic Resonance Imaging (MRI) is central to diagnosis and local staging of prostate cancer [1-6]. It is also increasingly used for treatment planning. With this increased use, non-radiologists may find more frequent occasion to view and evaluate the prostate and other structures on MRI. One fundamental task is recognizing the gland itself and its boundaries. Radiation oncologists desiring the most precise treatment target for their patients should use MRI, as it generally affords the most accurate view of prostate anatomy. Radiologists routinely measure gland volume and appreciate prostate boundaries to avoid missing intra-prostatic lesions for accurate MRI-ultrasound fusion for targeted biopsy [7]. Urologists often identify the prostate boundary when planning surgery. Physicians from multiple specialties may be interested in the relationship of the prostate to the nearby neurovascular bundle and in assessing proximity of cancer to the urethra [8, 9]. Further, outlining the urethra may be useful for clinicians, as for urologists the length of the membranous urethra is thought to relate to functional outcomes after surgery, and for radiation oncologists they may want to avoid overdosing the urethra [10-12].

Despite the numerous reasons that familiarity with prostate and urethra anatomy on MRI could be clinically relevant, there is little available information as to how well physicians treating prostate cancer can identify these structures. The need for accuracy is arguably greatest for radiation oncologists, who are tasked with delineating the prostate for precise treatment. The FLAME trial provides high-level evidence of improved oncologic outcomes with simultaneous focal radiotherapy boost to MRI-visible disease [13]. Secondary analysis of the same trial suggested urethra dose is associated with toxicity [10]. The urethra is not typically visible on CT scans used for simulation, meaning radiation oncologists need to use MRI. The MIRAGE trial found that reducing the radiotherapy planning treatment volume margin around the prostate from 4 mm to 2 mm significantly reduced toxicity to nearby genitourinary (GU) structures [14], suggesting that errors >2 mm in contouring the prostate itself could be clinically important. Meanwhile, physician variability on contouring the prostate on CT is subject to high variability and relatively large errors [15-17]. However, a recent survey of radiation oncologists highlighted lack of comfort with MRI as a substantial barrier to implementation of focal radiotherapy boost [13], and the ReIGNITE study revealed a lack of familiarity among some radiation oncologists with prostate anatomy on MRI [18, 19].

We sought to evaluate physician accuracy in contouring the prostate and urethra on MRI. Physicians who diagnose and/or treat prostate cancer were invited to participate in the Prostate and UREthra on MRI (PURE-MRI) study. We evaluated inter-physician variability in prostate and urethra contouring, as well as accuracy compared to a multidisciplinary panel's consensus.

Methods:

To evaluate physician contouring accuracy, we needed prostate MRI scans with reference standard for the prostate and urethra contours developed by experts. Participants should have formal clinical training in GU anatomy and experience treating patients with prostate cancer. And we needed to define appropriate and clinically relevant metrics to assess accuracy.

Patient Cases

Eligible patient cases had undergone prostate multiparametric MRI for known or suspected prostate cancer. A total of 4 patient cases included in this study underwent prostate multiparametric MRI for prostate cancer workup at University of California, San Diego (UCSD) Health between June 2023 to June 2024 (Table 1). One case had been chosen because it had been used as representative case in a previous study of artificial intelligence auto-segmentation tools [20]. Three additional cases were selected among the institutional database for their reasonable image quality and visualized prostate glands. These patients were of ages 67-84 years old and were found to have localized intermediate-risk or high-risk prostate cancer on biopsy.

Multidisciplinary consensus

Expert-defined contours were obtained to serve as consensus contours to compare with participant and auto-segmented contours. A multidisciplinary, multi-institution team of two genitourinary radiation oncologists (10 years' experience each) and two genitourinary radiologists (with 12 and 21 years' experience, respectively) created contours of the prostate in consensus for each of the patients on T_2-weighted MRI [20]. One of the panelists created initial contours on high-resolution axial T_2-weighted images (always viewed in all three planes), which were reviewed in panel meetings, slice by slice. High-resolution coronal and sagittal T_2-weighted acquisitions were available and viewed as needed to complement the axial volume. If any panel member judged the contour deviated > 1 mm from the true prostate boundary, the panel deliberated until unanimous agreement was met. Each slice case was reviewed at least twice. The same review procedures were followed for the urethra. As described previously [20], the panel adopted consensus ground rules to navigate around seminal vesicle tissue and the prostate apex. Likewise, the panel agreed on ground rules for how to contour the urethra. The prostatic urethra and membranous urethra were included. Wherever the urethra was not clearly visible on a given slice (often true at the mid-gland and part of the base of the prostate), the panel used all available anatomic information from the three planes to identify the most likely location. The urethra was always delineated as a continuous structure from the bladder neck to the prostatic apex and membranous urethra, until the most superior axial slice where the penile bulb was fully visible.

Participant Eligibility

Eligible participants were radiation oncologists, radiologists, or urologists who diagnose and/or treat prostate cancer. Clinical residents or fellows in the above specialties were also eligible if they had completed at least one prostate-focused clinical rotation. Study recruitment materials, communications, and procedures were approved by the UCSD Institutional Review Board (IRB). Participants were recruited via social media, email, and word-of-mouth in the genitourinary oncology community.

Participant Contours

Participants were randomly assigned 2 of the 4 patient cases on conventional, axial, T_2-weighted MRI. Contours of prostate and urethra structures were completed using MIM Cloud and MIM Zero Footprint software (MIM Software, Cleveland, OH). Instructions were provided as a pdf and as a video. We offered one-on-one guidance via teleconference to participants who had difficulty with the software or instructions. Participants were asked to contour the entire prostate. For the urethra, participants were asked to contour prostatic and membranous urethra. All participants were encouraged to complete contours for at least one patient case, with the option to complete more cases if willing.

Artificial Intelligence (AI) Auto-segmentation

For comparison with human contours, a validated prostate auto-segmentation AI tool [20] was used to produce prostate contours on all 4 of the patient cases. No AI tool was evaluated for urethra contours.

Assessment of accuracy and error

All participant contours were deidentified and compared to the consensus contours. Accuracy of participant prostate contours was assessed using Dice score of the entire prostate (1 indicates perfect overlap; 0 indicates no overlap). AI prostate contours were similarly assessed. To assess deviation from the expert consensus contour boundary, we measured participant under-segmentation via maximum deviation inside (mm) and over-segmentation via maximum deviation outside (mm), respectively. From these metrics, we also calculated the mean deviation error (mm) over the whole prostate boundary. To measure how accurately the superior and inferior extent were defined, we counted slice difference at the prostatic apex and base. This was calculated as the absolute difference in slices between most inferior axial expert contour and participant contour at the apex and similarly with the most superior axial contours at the base of the prostate. Finally, we measured absolute volume difference (%) from expert generated prostate volumes.

To assess accuracy of urethra contours, we compared the clinician generated contours with the expert consensus contours. We analyzed Dice score, volume overlap (%), and Hausdorff distance (mm). First, we reported these metrics along the full length of the urethra (intraprostatic and membranous urethra). We then repeated these analyses for the intraprostatic urethra segmented within the base, middle, and apex, as well as the isolated membranous urethra. We also measured the absolute membranous length difference (mm) compared to expert consensus contours.

Linear mixed effects models were used to evaluate potential factors influencing prostate and urethra contour accuracy. For these models, participants and the MRI patient cases were set as random effects. Fixed effects were set as physician specialty (radiation oncologist, radiologist, or urologist) and clinical experience (still in training, < 5 years, 5-10 years, and >10 years). GU sub-specialization was also set as a fixed effect with the following ordered categories: “Not specialized,” “partially specialized,” or “completely specialized” as self-reported by participants.

<u>Results:</u>

Cases

A total of 62 physicians from 11 countries participated, representing radiation oncology, radiology, and urology, with a range of sub-specialization and varying years of experience (Table 2). Most of the participants (n=46) completed 2 patient cases, some (n=13) completed only 1 patient case, and few (n=3) completed 3 patient cases. These clinicians produced a total of 224 structure segmentations (114 prostate and 110 urethra contours). 85 (38%) segmentations were done on case 4, 52 (23%) on case 3, 47 (21%) on case 2, and 40 (18%) on case 1.

Assessment of prostate contour accuracy

Overall, participant prostate contours had a median (minimum, maximum) Dice score of 0.92 (0.62, 0.95). Median max deviation error inside and outside for participant contours were 3.4 mm (1.0, 12.4) and 5.3 mm (2.4, 17.3), respectively. At the prostate apex, participant prostate contours had a median slice difference of 1 (0, 5). At the prostate base there was a median slice difference of 0 (0, 5). Participant prostate contour volume differed from expert contour volume by a median of 7.6% (0.1%, 48.2%) (Figure 2C). Among radiation oncologists, Dice score did not appear to vary with years of clinical experience (Figure 3A). Linear mixed effects models did not demonstrate significant, definitive relationships between prostate contour accuracy metrics with specialty, sub-specialization, or clinical experience (Supplementary Tables 1-5).

The AI auto-segmentation tool's contours had a median Dice score of 0.95 (0.94, 0.96). Other metrics of accuracy for auto-segmentation contours including slice differences at the prostate apex and base, and absolute percent volume differences from consensus contours were within range of participant contour metrics (Figure 2A-C).

Assessment of urethra contour accuracy

Urethra contours were left unmodified if participants made contiguous segmentations from the base of the bladder to the prostate apex and/or membranous urethra. For participants (n=4) who left some gaps in their urethra contours (e.g., contoured every other slice), the gaps were interpolated using MIM Software's default tool to allow for consistency in accuracy assessment. Clinician urethra contours had a median Dice score of 0.33 (0.03, 0.69) (Table 4). Urethra contours were also assessed by anatomic region (base, mid, apex, and membranous); contours drawn in the apex region had the highest median Dice score (Figure 4A). Median percent volume overlap of clinician urethra contours was 35.7% (3.0%, 95.5%). Similarly, participant urethra contours overlapped the most with expert urethra consensus contours within the apex (Figure 4B).

Hausdorff distance was calculated in segments relative to prostate region. If a participant left a segment of the prostate empty, we excluded their contour from analysis of that segment. We excluded 6 clinician contours missing urethra segmentation at the base and 30 clinician contours missing membranous urethra segmentation. Hausdorff distance for membranous urethra and intraprostatic urethra at the apex, middle, and base were 1.3 mm (0.7, 2.3), 1.3 mm (0.8, 2.2), 1.4 mm (0.9, 2.2), and 1.5 mm (0.6, 2.3), respectively (Figure 4C). Among completed membranous urethra contours (n=80), the median absolute difference in membranous urethra length (compared to the consensus contour) was 5.1 mm (0, 16.6) (Table 4). Linear mixed effects models did not

show substantial relationships between participant characteristics and urethral accuracy (Supplementary Tables 6-7).

Discussion:

We analyzed 114 contours of the prostate on MRI by 62 physician participants from 11 countries and found that they generally had excellent average agreement with a multidisciplinary consensus panel (median Dice score 0.92). Encouragingly, these results did not depend heavily on specialty, and inexperienced participants appeared to do about as well as more experienced subspecialists. Despite these overall promising results, though, there were some instances of poor agreement (e.g., Figure 1A) that could result in inadequate treatment of the prostate. Participants also typically had at least one error of over 5 mm and sometimes up to 17 mm, relative to the reference standard. Mean errors across the full prostate boundary were much smaller (median 1-2 mm). Median volume difference was less than 8%.

Similar to physician results, an AI auto-segmentation tool performed well for contouring the prostate. The AI tool achieved a Dice score of 0.94-0.96 for each of the four patient cases. The mean error was ≤1.6 mm for each patient case. There were some focal errors where the AI boundary deviated from the panel's consensus contour, typically by 3-4 mm, but this compares favorably to the human contours. The AI tool had no errors >5 mm, whereas human errors were seen as large as 17 mm. These accurate results are consistent with a previous validation study in a larger number and range of patient cases from multiple institutions and scanners [20]. While the AI tool could be improved, it is already performing at the level of a subspecialist physician.

In line with our findings, previous studies demonstrated excellent agreement between manual contours and gold-standard contours of the prostate on MRI in terms of Dice score [21]. However, though guidelines exist to assist with prostate segmentation accuracy, both intra- and inter-observer variations persist even when using the same imaging dataset [22, 23]. As a result, prostate manual segmentation comes with substantial uncertainty. In parallel, with the rapid emergence of artificial intelligence (AI) applications and widespread implementation of AI algorithms into medical imaging, auto-segmentation tools are rising. Other studies have also shown good performance of AI tools for the prostate, with a growing body of evidence demonstrating promise for integration of auto-segmentation tools to improve efficiency of clinical workflow [20, 24-27]. Such tools would also reduce the intra- and inter-physician variability reported previously[22, 23].

On the other hand, the urethra poses as a larger challenge as physicians struggled to delineate the urethra. This is relevant, as there is substantial international interest in sparing the urethra in hopes of reducing treatment toxicity [28-30]. Dice scores were very low, with a median of 0.33. The worst urethra contour barely touched the reference urethra (Dice score 0.03; Figure 1C), and even the best physician contour only achieved a modest Dice score of 0.69. One possibility is participants could have achieved poor Dice scores because they were conservatively over-contouring to encompass the urethra broadly. This appears not to be the case, though, as the median percentage of the consensus urethra encompassed by participants' contours was less than 36%, with all segments except the apex seeing at least one physician give 0% coverage. Regions of the prostatic urethra near the middle and base of the prostate had lower Dice scores

which could be due to the anatomic path of the urethra being more oblique as it passes through the prostate superiorly, which limits axial visualization. These results raise significant questions regarding the reliability of physician urethra contours. Studies reporting analysis of radiation dose-dependent toxicity are likewise suspect without careful central review of urethra contours.

Given the low bar of current human performance, an AI tool could be very useful for research (normal-tissue complication probability analyses) and even for clinical practice. Currently, we are working to develop a model that can achieve high accuracy and have invited several companies with existing tools to allow us to evaluate them [31]. These studies are left for future work. While we await validation and availability of suitable AI tools, we suggest more educational initiatives are warranted, perhaps through the major radiation oncology and radiology society meetings. There are no definitive guidelines for delineation of the urethra [32], and it is a challenging task. The multidisciplinary panel for the present study notes that the membranous and apical urethra are typically visible. The bladder neck is also typically visible, especially on sagittal views. The intraprostatic urethra in the mid-gland and base can be substantially more difficult and is sometimes not visible. The urethra generally sits between the two halves of the central gland, though benign prostatic hyperplasia nodules can cause significant deviation from midline in many patients. Finally, visible parts of the urethra must be connected to each other, allowing for some sensible interpolation. We are publishing here the panel consensus contours for all slices from one example patient case as an educational resource (Supplemental Table 8).

Other possibilities for delineating the urethra include voiding cystourethrography, retrograde urethrography, or transrectal ultrasonography [32]. Placement of a catheter will make the urethra readily visible but is invasive and distorts the urethral anatomy such that accuracy might require placement of the catheter for every radiation treatment, for example [33, 34]. Simpler surrogates for the urethra have shown promise and could be evaluated further [35]. Some centers use a 3D T_2-weighted acquisition (analogous to 3D FLAIR sometimes used for brain MRI) to help find the urethra. The multidisciplinary panel here evaluated images from several centers and concluded that there was not a clear benefit, as the axial reconstructions tend to be blurrier than 2D axial series due to the increased susceptibility of 3D acquisitions to motion artifact. Still, this may prove to be an effective strategy with more investigation. At least one study suggests micturition just prior to prostate MRI makes the urethra more visible [31]. This could be a viable approach, though most diagnostic imaging centers already suggest patients use the restroom prior to MRI for practical reasons (and MRI sim for prostate radiotherapy would often entail a full bladder).

Our study has some limitations. First, our study included only four patient cases, as we favored being able to directly compare multiple contours on the same case. Also, in isolation, Dice scores and other methods to evaluate spatial and volumetric structures lack specificity to understand if the errors measured are clinically significant [25]. Furthermore, there is hesitation to establish cut-off threshold values for these metrics as qualitative assessments by physicians may remain a valuable component [25]. Second, while outside the scope of this study, clinical use of prostate and urethra segmentation for radiotherapy or surgery has additional considerations, such as need for registration between imaging modalities and physiological changes of the prostate position between

scan and treatment. Further, we acknowledge that some anatomical variations or disease states may make outlining more challenging (e.g. peri-prostatic veins, large volume disease with ECE, utricle/Wolffian duct cysts, atrophic seminal vesicles, etc).

Conclusion

Regardless of clinical experience, specialty, or clinical focus, physicians were able to contour the prostate on MRI with typically (but not universally) excellent Dice scores (>0.90). An AI prostate segmentation tool performed at least as well as human physician participants. Contouring the urethra on MRI is more challenging, calling into question the feasibility of clinicians to adopt more urethral-sparing techniques for radiotherapy without more widespread education or development of more robust techniques.

Table 1. Acquisition parameters for T_2-weighted MRI sequences for patient cases used in this study. TR: repetition time. TE: echo time. FOV: field-of-view. FSE: fast spin echo. UCSD: University of California San Diego. For FOV, there were two sets listed as one of the patient cases had different matrix dimensions for each plane; the other three patient cases had the same matrix dimensions of 360 x 224 for all planes.

Scanner Characteristics	**Axial T_2**	**Sagittal T_2**	**Coronal T_2**
Pulse Sequence	FSE	FSE	FSE
TR (ms)	3276-3615*	2662-4684*	2662-3357*
TE (ms)	98-172*	98-173*	98-167*
FOV (mm)	160 x 160, 180 x 180	160 x 160, 180 x 180	160 x 160, 180 x 180
Matrix (resampled dimensions)	360 x 224, 400 x 256	360 x 224, 384 x 384	360 x 224, 400 x 400
Slices	32	26	26
Slice Thickness (mm)	3	3	3

** TR and TE reported as minimum and maximum range, as these measurements varied for each patient case.*

Table 2. Summary characteristics of participants from survey.

Characteristics	**Description**	**Frequency (%), (n=62)**
Country	Australia	5 (8%)
	Belgium	1 (2%)
	Brazil	1 (2%)
	Cyprus	2 (3%)
	Denmark	1 (2%)
	Germany	5 (8%)
	India	2 (3%)
	Spain	1 (2%)
	Switzerland	1 (2%)
	United Kingdom	6 (10%)
	United States	37 (60%)
Setting	Rural	1 (2%)
	Suburban	14 (23%)
	Urban	47 (76%)
Specialty	Radiation Oncologist	43 (69%)
	Radiologist	12 (19%)
	Urologist	7 (11%)
Genitourinary-Focused Practice	No	18 (29%)
	Partially	25 (40%)
	Completely	19 (31%)
Clinical Experience	Still in training	14 (23%)
	<5 years	12 (19%)
	5-10 years	11 (18%)
	> 10 years	25 (40%)

Table 3. Physician and AI prostate contour accuracy metrics, reported as median (minimum, maximum).

Prostate Accuracy Metric		**Physician Contours, (n=114),** *median (min, max)*	**AI Contours, (n=4),** *median (min, max)*
Dice Score	Whole	0.92 (0.62, 0.95)	0.95 (0.94, 0.96)
Slice Difference	Apex	1 (0, 5)	1.00 (0.75, 1.00)
	Base	0 (0, 5)	0
Error Deviation (mm)	Max inside	3.4 (1.0, 12.4)	3
	Max outside	5.3 (2.4, 17.3)	3.9 (3.1, 4.9)
	Mean	1.6 (0.9, 3.9)	1.2 (1.1, 1.6)
Volume Difference (%)	Whole	7.6 (0.1, 48.2)	4.0 (3.4, 7.0)

Table 4. Physician urethra contour accuracy metrics, reported as median (minimum, maximum). Hausdorff distance was calculated only with urethra structures that included contours drawn in that region. For example, there were 104 urethra structures that had contours that included the base region, and there were only 80 structures that included contours past the apex into the membranous region. Similarly, membranous length difference was calculated only for urethra structures that included contours in the membranous region.

Urethra Accuracy Metric		**Physician urethra contours, (n=110),** *median (min, max)*
Dice Score	Whole	0.33 (0.03, 0.69)
	Base	0.23 (0, 0.68)
	Mid	0.27 (0, 0.68)
	Apex	0.49 (0.07, 0.79)
	Membranous	0.30 (0, 0.77)
Volume Overlap (%)	Whole	35.7 (3.0, 95.5)
	Base	28.7 (0, 100)
	Mid	35.2 (0, 100)
	Apex	61.8 (4.1, 100)
	Membranous	29.5 (0, 100)
Hausdorff Distance (mm)	Base	1.5 (0.6, 2.3), *n=104*
	Mid	1.4 (0.9, 2.2)
	Apex	1.3 (0.8, 2.2)
	Membranous	1.3 (0.7, 2.3), *n=80*
Membranous Length Difference (mm)		5.1 (0, 16.6), *n=80*

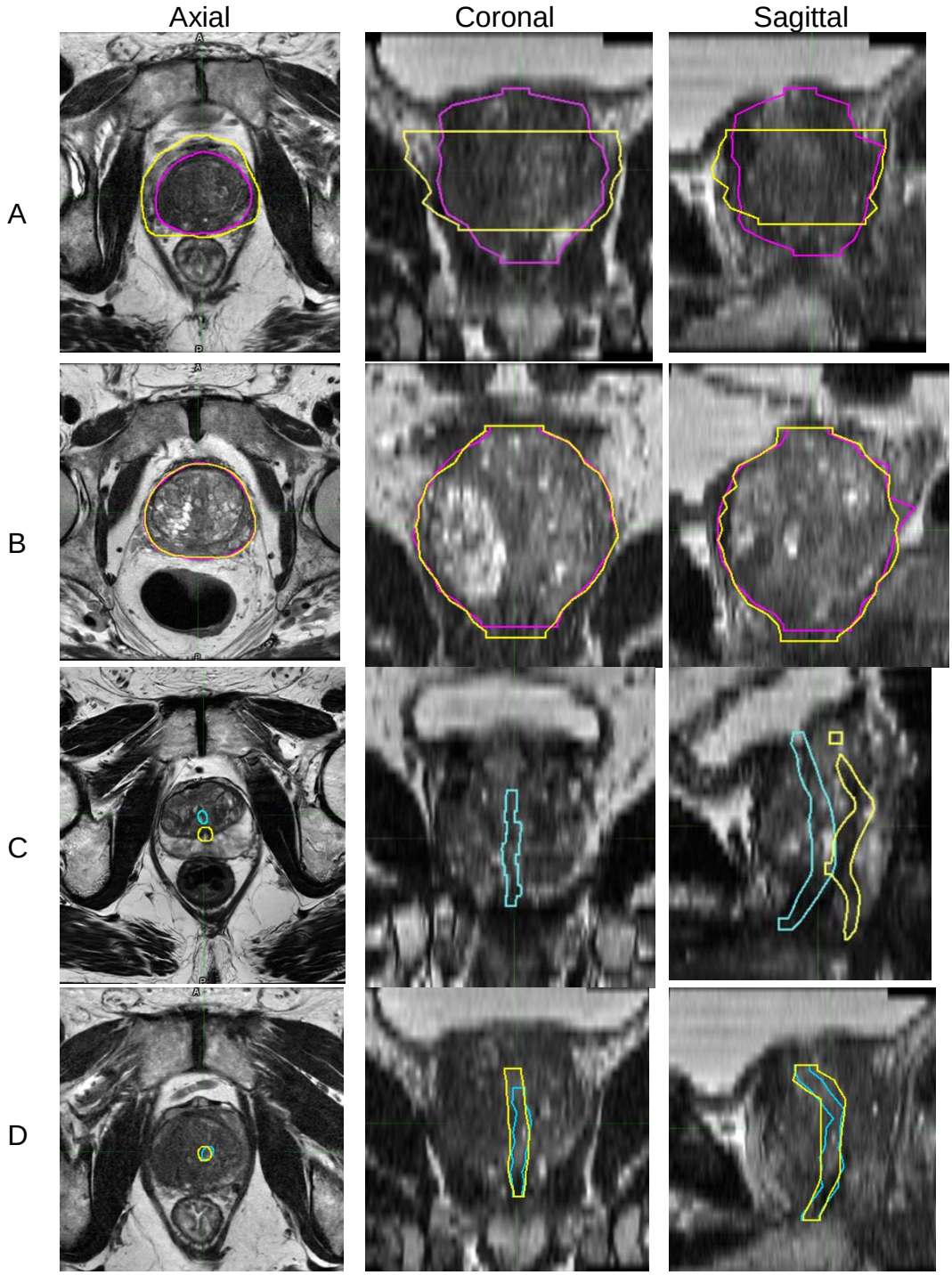

Figure 1. Examples of physician prostate and urethra contours overlayed with expert consensus contours per case on axial, coronal, and sagittal T_2-weighted MRI. Outlined in yellow were contours that were generated by participant. Outlined in magenta and teal were expert defined prostate and urethra, respectively. 1A is an example of physician prostate contours with poor accuracy as Dice score, mean error deviation, and volume difference were 0.62, 3.9 mm, and 39%, respectively. 1B is an example of high accuracy with Dice score, mean error deviation, and volume difference of 0.95, 1.1

mm, and 4%, respectively. In 1C, physician urethra contours had poor accuracy and overlap with Dice score of 0.03 and volume overlap of 3%. In 1D, these contours had greater Dice score of 0.69 and volume overlap of 85%.

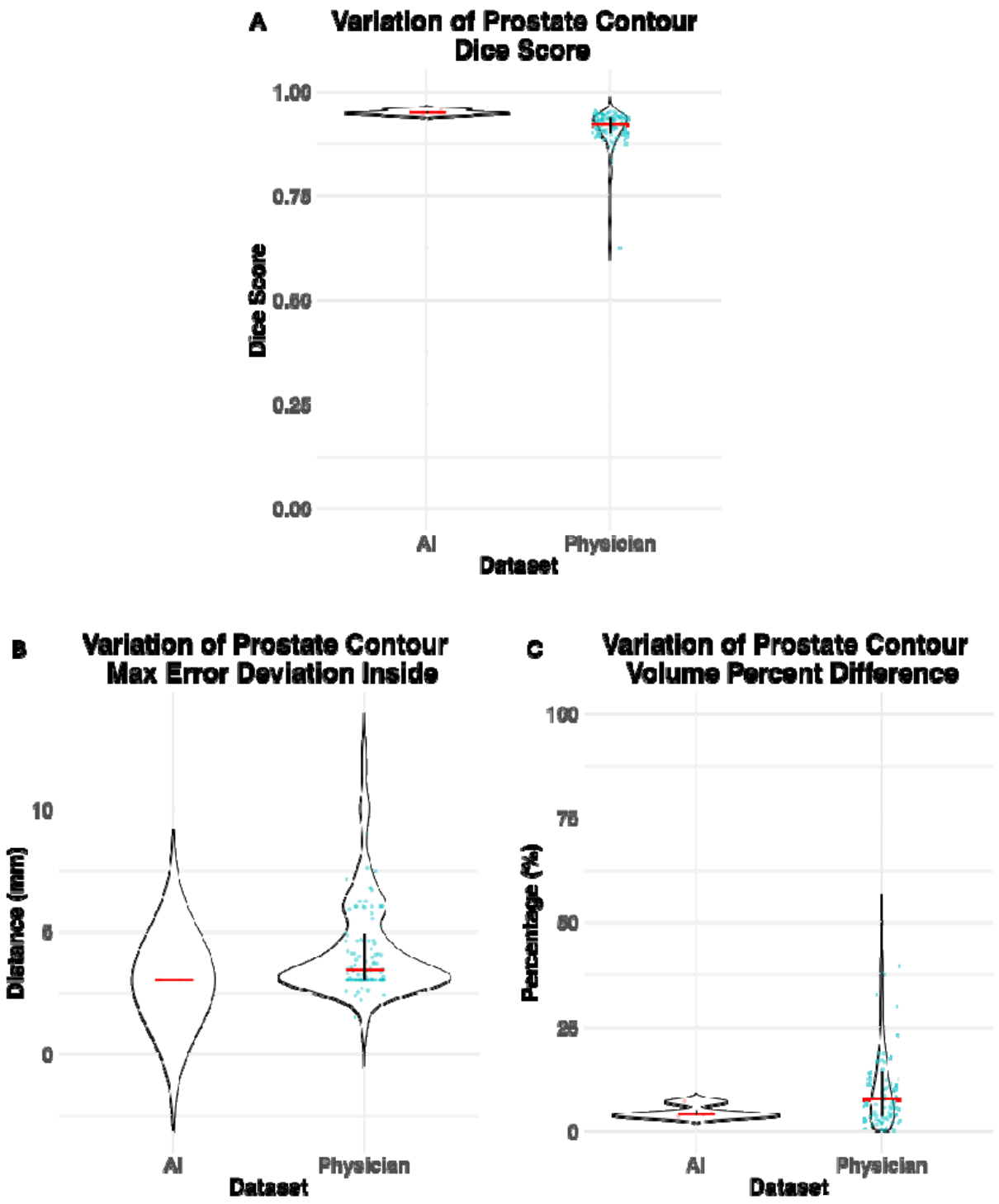

Figure 2. Variation of physician and AI prostate contour accuracy metrics. 2A shows the variation of physician and AI prostate Dice score. 2B shows the variation of max error deviation inside (or under-segmentation from expert consensus contour boundary). 2C

shows variation of volume percentage difference. The median is represented with the red bar and the IQR is represented with the black bar.

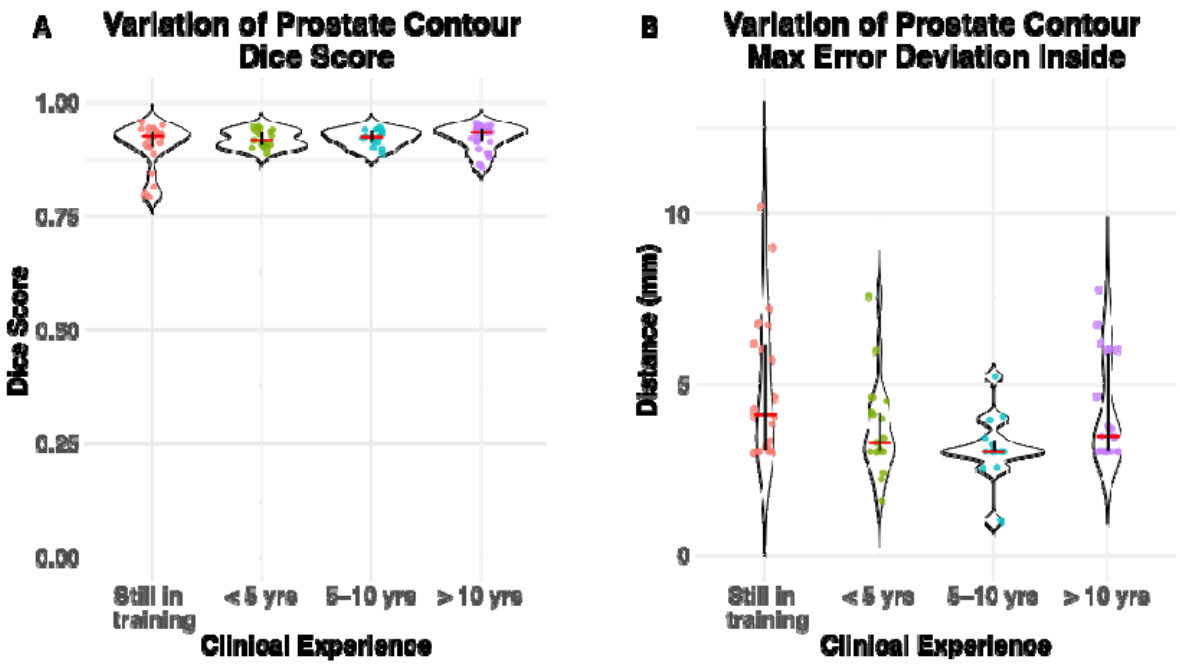

Figure 3. Variation of prostate contour accuracy metrics of radiation oncologists stratified by years of clinical experience. 3A shows the variation of Dice score among radiation oncologists by clinical experience. 3B shows the variation of max error deviation inside (or under-segmentation from expert consensus contour boundary) among radiation oncologists by clinical experience. The median is represented with the red bar and the IQR is represented with the black bar. Yrs= years.

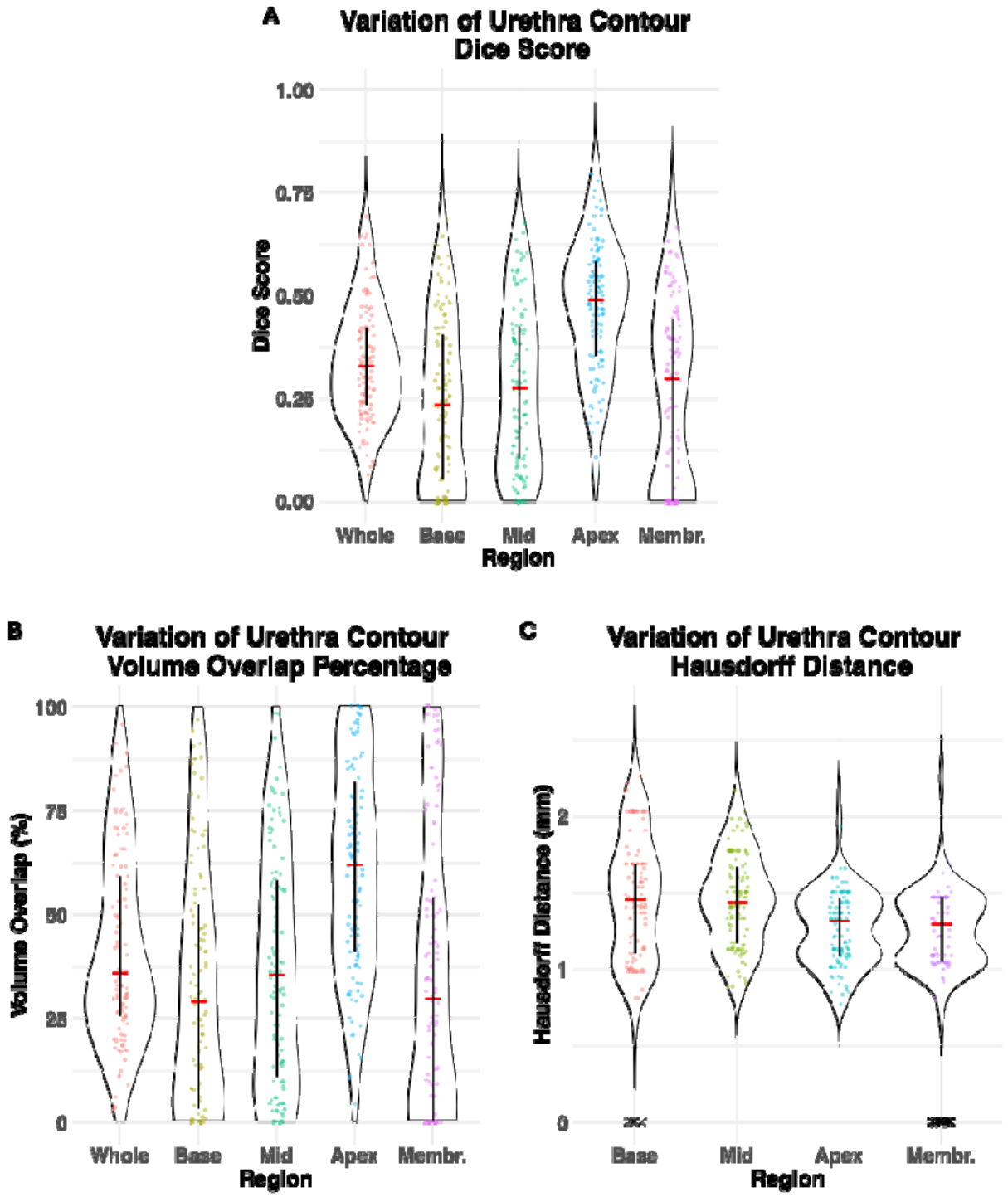

Figure 4. Variation of urethra contour accuracy metrics. 4A shows variation of urethra contour Dice score relative to anatomical prostate region. 4B shows variation of physician urethra contour volume overlap percentage with expert consensus contour relative to anatomical prostate region. 4C shows urethra contour Hausdorff distance per anatomical prostate region. The x's represent excluded urethra contours, as these

physician contours did not include segmentations in these anatomic regions. Membr.= Membranous.

References

1. Kasivisvanathan, V., et al., *MRI-Targeted or Standard Biopsy for Prostate-Cancer Diagnosis.* New England Journal of Medicine, 2018-05-10. **378**(19).
2. Ahmed, H.U., et al., *Diagnostic accuracy of multi-parametric MRI and TRUS biopsy in prostate cancer (PROMIS): a paired validating confirmatory study.* The Lancet, 2017/02/25. **389**(10071).
3. Eklund, M., et al., *MRI-Targeted or Standard Biopsy in Prostate Cancer Screening - PubMed.* The New England journal of medicine, 09/02/2021. **385**(10).
4. Ahdoot, M., et al., *MRI-Targeted, Systematic, and Combined Biopsy for Prostate Cancer Diagnosis.* New England Journal of Medicine, 2020-03-05.
5. Rouvière, O., et al., *Use of prostate systematic and targeted biopsy on the basis of multiparametric MRI in biopsy-naive patients (MRI-FIRST): a prospective, multicentre, paired diagnostic study - PubMed.* The Lancet. Oncology, 2019 Jan. **20**(1).
6. Hugosson, J., et al., *Results after Four Years of Screening for Prostate Cancer with PSA and MRI - PubMed.* The New England journal of medicine, 09/26/2024. **391**(12).
7. Dorfinger, J., et al., *MRI/ultrasound fusion biopsy of the prostate compared to systematic prostate biopsy – Effectiveness and accuracy of a combined approach in daily clinical practice.* European Journal of Radiology, 2022/09/01. **154**.
8. Tan, N., et al., *Radical prostatectomy: value of prostate MRI in surgical planning.* Abdom Imaging, 2012. **37**(4): p. 664-74.
9. Park, B.H., et al., *Influence of magnetic resonance imaging in the decision to preserve or resect neurovascular bundles at robotic assisted laparoscopic radical prostatectomy.* J Urol, 2014. **192**(1): p. 82-8.
10. Groen, V.H., et al., *Urethral and bladder dose-effect relations for late genitourinary toxicity following external beam radiotherapy for prostate cancer in the FLAME trial - PubMed.* Radiotherapy and oncology : journal of the European Society for Therapeutic Radiology and Oncology, 2022 Feb. **167**.
11. Coakley, F.V., et al., *Urinary continence after radical retropubic prostatectomy: relationship with membranous urethral length on preoperative endorectal magnetic resonance imaging - PubMed.* The Journal of urology, 2002 Sep. **168**(3).
12. Paparel, P., et al., *Recovery of urinary continence after radical prostatectomy: association with urethral length and urethral fibrosis measured by preoperative and postoperative endorectal magnetic resonance imaging - PubMed.* European urology, 2009 Mar. **55**(3).
13. Kerkmeijer, L.G.W., et al., *Focal Boost to the Intraprostatic Tumor in External Beam Radiotherapy for Patients With Localized Prostate Cancer: Results From the FLAME Randomized Phase III Trial.* J Clin Oncol, 2021. **39**(7): p. 787-796.
14. Kishan, A.U., et al., *Magnetic Resonance Imaging-Guided vs Computed Tomography-Guided Stereotactic Body Radiotherapy for Prostate Cancer: The MIRAGE Randomized Clinical Trial - PubMed.* JAMA oncology, 03/01/2023. **9**(3).

15. Chung, E., et al., *Expansion/de-expansion tool to quantify the accuracy of prostate contours - PubMed.* International journal of radiation oncology, biology, physics, 05/01/2012. **83**(1).
16. McLaughlin, P.W., et al., *Radiographic and anatomic basis for prostate contouring errors and methods to improve prostate contouring accuracy - PubMed.* International journal of radiation oncology, biology, physics, 02/01/2010. **76**(2).
17. Gao, X.-S., et al., *Pathological analysis of clinical target volume margin for radiotherapy in patients with esophageal and gastroesophageal junction carcinoma - PubMed.* International journal of radiation oncology, biology, physics, 02/01/2007. **67**(2).
18. Lui, A.J., et al., *ReIGNITE Radiation Therapy Boost: A Prospective, International Study of Radiation Oncologists' Accuracy in Contouring Prostate Tumors for Focal Radiation Therapy Boost on Conventional Magnetic Resonance Imaging Alone or With Assistance of Restriction Spectrum Imaging.* Int J Radiat Oncol Biol Phys, 2023. **117**(5): p. 1145-1152.
19. Zhong, A.Y., et al., *Use of focal radiotherapy boost for prostate cancer: radiation oncologists' perspectives and perceived barriers to implementation.* Radiat Oncol, 2023. **18**(1): p. 188.
20. Song, Y., et al., *Precise prostate contours: setting the bar and meticulously evaluating AI performance.* medRxiv, 2024-10-22.
21. Pathmanathan, A.U., et al., *Comparison of prostate delineation on multimodality imaging for MR-guided radiotherapy.* Br J Radiol, 2019. **92**(1095): p. 20180948.
22. Patrick, H.M., L. Souhami, and J. Kildea, *Reduction of inter-observer contouring variability in daily clinical practice through a retrospective, evidence-based intervention.* Acta Oncol, 2021. **60**(2): p. 229-236.
23. Jameson, M.G., et al., *A review of methods of analysis in contouring studies for radiation oncology.* J Med Imaging Radiat Oncol, 2010. **54**(5): p. 401-10.
24. Rong, Y., et al., *NRG Oncology Assessment of Artificial Intelligence Deep Learning-Based Auto-segmentation for Radiation Therapy: Current Developments, Clinical Considerations, and Future Directions.* Int J Radiat Oncol Biol Phys, 2024. **119**(1): p. 261-280.
25. Sherer, M.V., et al., *Metrics to evaluate the performance of auto-segmentation for radiation treatment planning: A critical review.* Radiother Oncol, 2021. **160**: p. 185-191.
26. Cha, E., et al., *Clinical implementation of deep learning contour autosegmentation for prostate radiotherapy.* Radiother Oncol, 2021. **159**: p. 1-7.
27. Aldoj, N., et al., *Automatic prostate and prostate zones segmentation of magnetic resonance images using DenseNet-like U-net.* Sci Rep, 2020. **10**(1): p. 14315.
28. Guévelou, J.L., et al., *Urethra-sparing prostate cancer radiotherapy: Current practices and future insights from an international survey.* Clin Transl Radiat Oncol, 2025. **51**: p. 100907.
29. Martin, J.M., et al., *Mechanisms, mitigation, and management of urinary toxicity from prostate radiotherapy - PubMed.* The Lancet. Oncology, 2022 Dec. **23**(12).

30. Pham, J., et al., *Evaluation of T2-Weighted MRI for Visualization and Sparing of Urethra with MR-Guided Radiation Therapy (MRgRT) On-Board MRI - PubMed.* Cancers, 07/16/2021. **13**(14).
31. Yoshimura, T., et al., *Visualizing the urethra by magnetic resonance imaging without usage of a catheter for radiotherapy of prostate cancer.* Physics and Imaging in Radiation Oncology, 2021/04/01. **18**.
32. Kataria, T., et al., *Simple diagrammatic method to delineate male urethra in prostate cancer radiotherapy: an MRI based approach.* Br J Radiol, 2016. **89**(1068): p. 20160348.
33. Litzenberg, D.W., et al., *Changes in prostate orientation due to removal of a Foley catheter - PubMed.* Medical physics, 2018 Apr. **45**(4).
34. Dekura, Y., et al., *The urethral position may shift due to urethral catheter placement in the treatment planning for prostate radiation therapy - PubMed.* Radiation oncology (London, England), 12/12/2019. **14**(1).
35. Ratnakumaran, R., et al., *Developing and validating a simple urethra surrogate model to facilitate dosimetric analysis to predict genitourinary toxicity.* Clinical and Translational Radiation Oncology, 2024/05/01. **46**.